

# Atomistic Modeling for Boron Activation Enhancement using Silicon pre implant technique

Joong - sik Kim, Young-kyu Kim, Kwan-sun Yoon and Taeyoung Won

Department of Electrical Engineering, School of Engineering, Inha University  
National IT Research Center for Computational Electronics  
253 Yonghyun-dong, Nam-gu, Incheon 402-751, Korea  
Phone: +82-32-875-7436 Fax: +82-32-862-1350 E-mail: { [kjs, twon@hse.inha.ac.kr](mailto:kjs.twon@hse.inha.ac.kr) }

## Abstract

In this paper, we report our KMC study on the enhancement of boron activation by Si pre-implant process. We investigated the activation of boron during thermal process after the silicon pre-implant and found that the activation has been enhanced due to the presence of a vacancy rich region close to the surface. In this paper, we also report our numerical study on the effect of the silicon pre-implant (PAI) on the reduction of boron transient enhanced diffusion (TED).

## 1. Introduction

With increasingly stringent requirement on the depth scaling of the source/drain junction in CMOS devices, pre-amorphization has also been used prior to low energy implant to generate shallower junction depth.[1-3]

It is well known that boron atoms experience so-called transient enhanced diffusion (TED) during post-implant annealing process due to their interaction with the silicon interstitials and that the activation of dopants is limited by the thermal solid solubility. [4-6] High energy ion implantation provide a unique method to separate the spatial distribution vacancy-rich region close to the surface [6]. There are some technical reports on the mechanism of diffusion in silicon pre implant relying on the macroscopic diffusion model. For better understanding the physics of boron diffusion, however, an atomistic modeling approach is essential due to the inherent limit of the continuum model for nano-scale devices. In this work, we investigated the effect of Si pre-implantation on the low energy B implant and boron activation enhancement during the post-implant annealing process using kinetic Monte Carlo (KMC) approach.

## 2. Kinetic Monte Carlo Implementation

In the KMC method, a physical system, which consists of many possible events, evolves as a series of independent event occurring. Each event has its own event rate. Event rate is calculated from the equation (1). Here,  $E_b$  presents

the migration energy for the barrier against the jump event of the mobile species or a binding energy for clusters. In addition,  $\nu_0$  is the attempt frequency, which is simply the vibration frequency of the atoms. Typically, the attempt frequency is of the order of 1/100 fs. These parameters can be obtained from *ab-initio* calculation or experimental data [7].

$$\nu = \nu_0 \exp\left(\frac{-E_b}{K_B T}\right). \quad (1)$$

Our problem is the consideration about the thermally activated events in a thermal-annealing simulation after ion implantation. If the probability for the next event to occur is independent of the previous history, and the same at all times, the transition probability will be a constant, which is called Poisson process. To derive the time dependence, we can consider a single event with a uniform transition probability  $r$ . Let  $f$  be the transition probability density, which gives the probability rate at which the transition occurs at time  $t$ . The change of  $f(t)$  over some short time interval  $dt$  is proportional to  $r$ ,  $dt$  and  $f$ , because  $f$  gives the probability density that the physical system still remains at time  $t$ .

$$df(t) = -rf(t)dt. \quad (2)$$

Further, the solution is given by the following boundary conditions.

$$f(t) = re^{-rt}, f(0) = r. \quad (3)$$

Therefore, the simulation time is updated for ( $t = t + \Delta t$ ) according to event rates as follows, because an ensemble of independent Poisson processes will behave as one large Poisson process:

$$\Delta t = -\frac{\ln u}{R}. \quad (4)$$

Here,  $u$  is a random number and  $R$  is the total sum of all possible event rates. We select an event according to the event rates, and KMC is suitable to simulate non-uniform time evolution processes. Figure 1 shows above work flows shortly. Cluster model is important in investigating TED.

Clusters, including silicon interstitial clusters ( $I_n$ ), vacancy cluster ( $V_n$ ) and boron silicon complex ( $B_m I_n$ ) are defined as the compound of single particle. All the combination actions of clusters are as follow:



where for  $I_n$  and  $V_n$ ,  $n < 100$  and for  $B_m I_n$ ,  $n < 5$  and  $m < 5$ . The annihilation and combination are assumed to occur whenever two concerned particles are close enough to each other. To obtain coordinates of all point defects and dopants with Ge PAI, we used BCA code (UT-MARLOWE 6.0). Obtained profile of interstitials, vacancy, and boron with Ge PAI is imported to KMC simulator for annealing process. Also, simulation box size is defined as 60 x 60 x 600 nm for annealing process.

#### 4. Experimental Design

In order to investigate silicon pre-implantation effect, Si implantation is performed with dosage of  $3 \times 10^{14}/\text{cm}^2$  and with implantation energy of 200keV. Further, B implantation is performed with dosage of  $4.5 \times 10^{15}/\text{cm}^2$  and implantation energy 2keV, followed by an annealing process is performed at 790 C for 18 sec.

#### 5. Results and discussion

Figure 1 is a diagram illustrating the comparison between the Si pre-implant boron profile with non silicon pre-implant boron profile. Figure 1 demonstrates that boron tail has been tremendously reduced for the junction due to the silicon pre-implant. It has been reported that this phenomenon is due to the defect imbalance [7]. It has also been reported that one of the reasons for the boron activation enhancement is due to vacancy rich region by high energy ion implant. In order to confirm the above-mentioned explanation, we performed some simulations using KMC code. First of all, we performed the diffusion simulation using KMC with same spatial distribution of interstitial and vacancy. Figure 2 shows as-implant profile of interstitial and vacancy, which has an identical spatial distribution. Thereafter, we simulate annealing process with I-V profile which have vacancy rich region. Figure 3 shows as-implant profile of interstitial and vacancy which has a vacancy rich region.

In order to confirm boron activation enhancement, we simulated boron diffusion during the annealing process

using above two I V profiles. Also we calculated substitutional boron concentration. Figure 4 shows the boron substitutional profile in terms of implant and annealing time. In this figure, we can observe that more boron is activated in the case of vacancy rich region than no vacancy rich region. From this results, we can conclude that enhancement of boron activation is due to surface vacancy rich region. Figure 5 shows the boron total, substitutional, complex profiles. In this figure, we observe that there exists a difference in total profiles with I-profiles in the boron complex region. Therefore, we can also conclude that non activated boron exists as boron complexes. In our KMC simulations, the parameters were obtained either from *ab-initio calculation* or from experimental data. Figure 7 shows the migration and binding energies employed in this study.

#### 6. Summary

In this work, the enhancement of boron activation has been numerically investigated in the silicon pre-implanted silicon substrate, which has a vacancy rich region in the atomistic scale. Our KMC simulation reveals that boron activation enhancement seems to be due to the presence of a vacancy rich region. Also, we can conclude that non-activated boron exists as boron complex. Our KMC study convinces us that these techniques are useful for solving problem of boron activation limit due to solid solubility.

#### Acknowledgements

This research was supported by the MIC(Ministry of Information and Communication), Korea, under the ITRC(Information Technology Research Center) support program supervised by the IITA(Institute of Information Technology Advancement)" (IITA-2006-C109006030030).

#### References

- [1] H. S. Park, K. Jeong, H. W. Suh, H. J. Jung and W. K. Choi, J. Korean Phys. Soc. **44**, 1594 (2004).
- [2] A. Agarwal, D. J. Eaglesham, H. -J. Gossmann, L. Pelaz, S. B. Herner, D. C. Jacobson, T. E. Haynes, Y. Erokhin and R. Simonton, IEEE International Electron Devices Meeting, 467 (1997), Washington DC, USA.
- [3] L. Prlaz, G. H. Gilmer, V. C. Venezia, H. -J. Gossmann, M. Jaraiz and J. Barbolla, Appl. Phys. Lett. **74**, 2017 (1999).
- [4] P.M. Fahey, P. B. Griffin, and J. D. Plummer, Rev Mod. Phys. **61**, 289(1989)
- [5] P. A. Stolk, H-J. Gossmann, D. J. Eaglesham, D. C. Jacobson, C. S. Rafferty, G. H. Gilmer, M. Jaraiz, J. M. Poate, H. S. Luftman, and T. E. Haynes, J. Appl. Phys. **81**, 6031 (1977)
- [6] A. Agarwal, H-J. Gossmann, D. J. Eaglesham, S. B. herner, A. T. Fiory, and T. E. Haynes, Appl. Phys. Lett. **74**, 2435(1999)
- [7] M. Tang, L. Colombo, J. Zhu and T. Diaz de la Rubia, Phys.

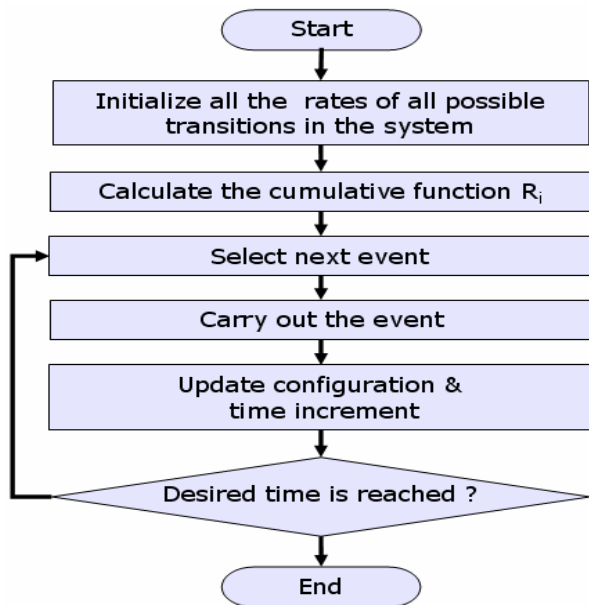


Fig. 1 Work flow of the KMC calculation.

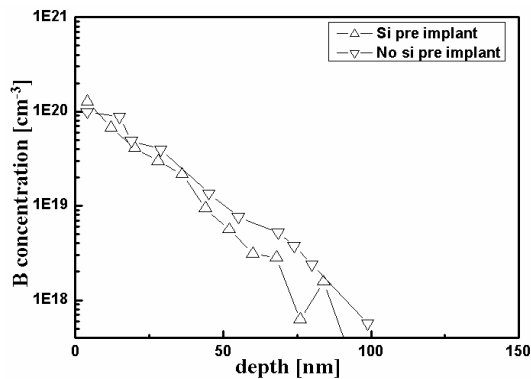


Fig. 2 Comparison si pre-implant with no si pre-implant data and reducing TED effect; boron 2 keV,  $4.5 \times 10^{14}/\text{cm}^2$ , silicon 200 keV,  $3 \times 10^{15}/\text{cm}^2$  and  $790^\circ\text{C}$  18s (RTA).

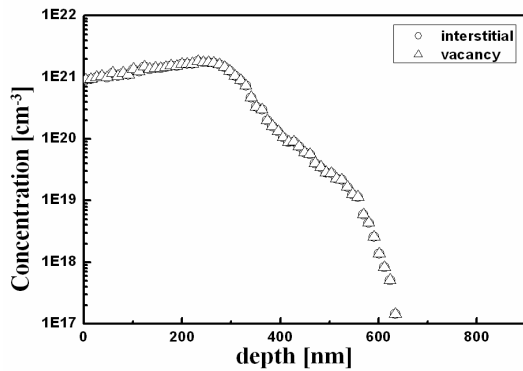


Fig. 3 Interstitial and vacancy as implanted profile ; Si 200keV,  $3 \times 10^{15}/\text{cm}^2$ ; No vacancy rich region.

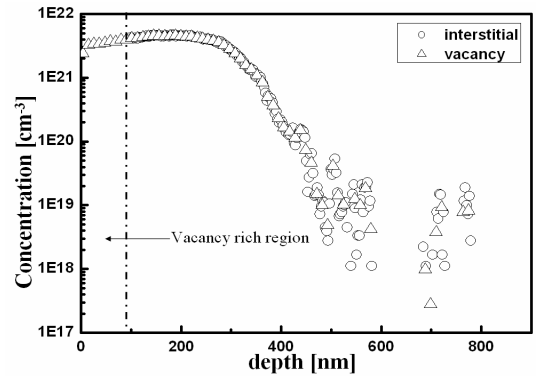


Fig. 4 Interstitial and vacancy as implanted profile ; Si 200keV,  $3 \times 10^{15}/\text{cm}^2$ ; Vacancy rich region.

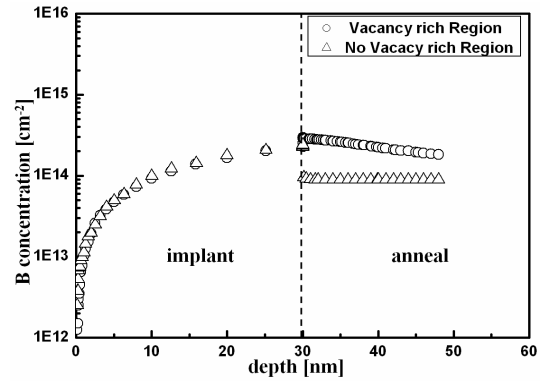


Fig. 5 Simulated time evolution of the substitutional boron ; boron 2 keV,  $4.5 \times 10^{14}/\text{cm}^2$ , silicon 200 keV,  $3 \times 10^{15}/\text{cm}^2$  and  $790^\circ\text{C}$  18s (RTA).

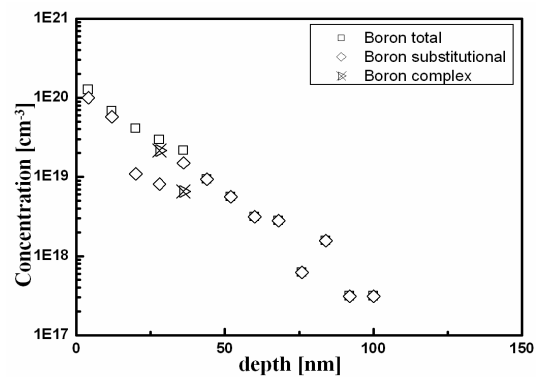


Fig. 6 This figure shows boron total, substitutional, complex profiles; boron 2 keV,  $4.5 \times 10^{14}/\text{cm}^2$ , silicon 200 keV,  $3 \times 10^{15}/\text{cm}^2$  and  $790^\circ\text{C}$  18s (RTA).

	$B_2I_3$ =-6.0	$B_3I_3$ =-8.0	$B_4I_3$ =-8.5
$BI_2$ =-3.3	$B_2I_2$ =-4.6	$B_3I_2$ =-6.0	$B_4I_2$ =-6.5
	$B_2I$ =-1.6	$B_3I$ =-3.6	$B_4I$ =-4.0
	$B_2$ =0.8	$B_3$ =0.8	$B_4$ =0.8

Fig. 7 Migration and binding energies of  $B_mI_n$  clusters use in this work.